MESSAGE PASSING-BASED COOPERATIVE LOCALIZATION WITH EMBEDDED PARTICLE FLOW

Lukas Wielandner[1,2], *Erik Leitinger*[1], *Florian Meyer*[3], *Bryan Teague*[4], *and Klaus Witrisal*[1,2]

[1]Graz University of Technology, Graz, Austria
[2]Christian Doppler Laboratory for Location-Aware Electronic Systems, Graz, Austria
[3]University of California San Diego, La Jolla, CA
[4]MIT Lincoln Laboratory, Lexington, MA

ABSTRACT

Cooperative localization is an enabling technology for the IoT that will introduce innovative services for modern convenience and public safety. Particle-based belief propagation (BP) is a state-of-the-art method for cooperative localization. However, in large and dense cooperative localization networks, particle-based BP suffers from particle degeneracy. In this paper, we propose a new method that combines particle-based BP and particle flow (PF) and can avoid this detrimental effect. To perform operations on the graph effectively, particles are moved towards regions of high likelihood based on the solution of a partial differential equation. We show that the proposed PF-BP algorithm can significantly outperform conventional particle-based BP in accuracy and runtime.

Index Terms— Cooperative localization, belief propagation, particle flow.

1. INTRODUCTION

The Internet of Things (IoT) will be formed by a large number of densely deployed wireless devices and will provide new location-aware services [1–11]. Cooperative localization methods aim to estimate the location of agents in a wireless sensor network. Promising algorithmic approaches for cooperative localization are based on the framework of factor graphs, and belief propagation (BP) [1–3], which can provide accurate solutions in high-dimensional Bayesian estimation problems efficiently. Here, message-passing on a factor graph based on the rules of the sum-product-algorithm (also known as BP) is performed to compute approximations ("beliefs") of the marginal posterior probability density functions (PDFs) of agent positions [1, 2]. Often, particle-based implementations are used to cope with multimodal distributions [2, 3]. A common strategy to avoid particle degeneracy is to construct or compute accurate proposal densities [2, 12, 13]. Recently, particle flow (PF) [14, 15] was considered to be used as an accurate proposal distribution for estimation problems in high-dimensions with highly informative likelihood functions. In particular, it was applied to multi-sensor localization [16, 17] and time-difference-of-arrival-based multi-target tracking [18, 19].

This work was supported in part by the Christian Doppler Research Association; the Austrian Federal Ministry for Digital and Economic Affairs; the National Foundation for Research, Technology, and Development; SES imagotag; and the Under Secretary of Defense for Research and Engineering under Air Force Contract No. FA8702-15-D-0001.

This work aims at improving the localization performance of Bayesian cooperative localization in large-scale networks. As most state-of-the-art techniques for cooperative localization, our approach is based on BP. PF is used to compute the messages of the loopy BP update steps. It enables the motion of particles towards regions of high likelihood and leads to an accurate approximation of the beliefs of agent locations with a relatively small number of particles. The main contributions of this paper are as follows.

- We introduce a Bayesian estimation method that combines BP with PF to avoid particle degeneracy in cooperative localization.
- We evaluate the estimation performance and runtime of the proposed method in large-scale cooperative localization scenarios with up to 200 agents.

Our numerical simulations demonstrate that the proposed BP-PF algorithm can significantly outperform conventional particle-based BP regarding positioning accuracy and runtime.

1.1. Notation

Random variables are denoted by sans serif, upright fonts, and their realizations by serif italic fonts. For example, a random variable is given as x and its realization as x. Vectors are denoted by bold lowercase letters and matrices in bold uppercase letters. The Euclidean norm of a vector $\boldsymbol{x}$ is indicated by $\|\boldsymbol{x}\|$ and its transpose by $\boldsymbol{x}^{\mathrm{T}}$. The mean value of a vector is denoted as $\bar{\boldsymbol{x}}$. The cardinality of a set $\mathcal{C}$ is defined as $|\mathcal{C}|$.

2. SYSTEM MODEL

We consider a set of static cooperating agents $\mathcal{C}$ with unknown positions and a set of anchors $\mathcal{A}$ with known positions. The number of agents and anchors is indicated by the cardinality of $\mathcal{C}$ and $\mathcal{A}$ respectively. We define two types of measurements: (i) measurements between anchors and agents $\tilde{\mathsf{z}}_{a,i}$ with $a \in \mathcal{A}$ and $i \in \mathcal{C}$ and (ii) measurements in-between agents $\underline{\mathsf{z}}_{i,j}$ with $i \in \mathcal{C}$ and $j \in \mathcal{D}_i$ where $\mathcal{D}_i \subseteq \mathcal{C}$ is the set of agents that cooperate with agent i. The stacked vector of all anchor measurements is written as $\tilde{\mathbf{z}} = [\tilde{\mathsf{z}}_{1,1}\ \tilde{\mathsf{z}}_{1,2}\ \ldots\ \tilde{\mathsf{z}}_{1,|\mathcal{C}|}\ \tilde{\mathsf{z}}_{2,1}\ \ldots\ \tilde{\mathsf{z}}_{|\mathcal{A}|,|\mathcal{C}|}]^{\mathrm{T}}$ which can also be written as $\tilde{\mathbf{z}} = [\tilde{\mathsf{z}}_{a,i}]_{a\in\mathcal{A},i\in\mathcal{C}}$. The stacked vector of all measurements in-between agents is given as $\underline{\mathbf{z}} = [\underline{\mathsf{z}}_{i,j}]_{i\in\mathcal{C},j\in\mathcal{D}_i}$. Each node (agent or anchor) has a fixed position which does not vary with time. The state of the ith agent, denoted $\mathbf{x}_i \in \mathbb{R}^2$ is defined as $\mathbf{x}_i = [\mathsf{x}_i\ \mathsf{y}_i]^{\mathrm{T}}$.

The anchor states are defined in the same manner, however, they are assumed to be known. The vectors $\mathbf{x}$ and $\mathbf{z}$ denote the stacked vectors of all agent and anchor states and all measurements (between agents and anchors and agents and agents) respectively, where $\mathbf{x} = [\mathbf{x}_1^{\mathrm{T}} \ \dots \ \mathbf{x}_{|\mathcal{C}|}^{\mathrm{T}}, \mathbf{x}_{|\mathcal{C}|+1}^{\mathrm{T}} \ \dots \ \mathbf{x}_{|\mathcal{C}|+|\mathcal{A}|}^{\mathrm{T}}]^{\mathrm{T}}$ and $\mathbf{z} = [\tilde{\mathbf{z}}^{\mathrm{T}} \ \underline{\mathbf{z}}^{\mathrm{T}}]^{\mathrm{T}}$. The joint posterior PDF is given as

$$f(\boldsymbol{x}|\boldsymbol{z}) \propto f(\boldsymbol{z}|\boldsymbol{x})f(\boldsymbol{x}) \tag{1}$$

with the joint likelihood $f(\boldsymbol{z}|\boldsymbol{x})$ and the prior of all agent states $f(\boldsymbol{x})$. Using common assumptions [1], (1) can be factorized as

$$f(\boldsymbol{x}|\boldsymbol{z}) \propto \bigg(\prod_{i\in\mathcal{C}} f(\boldsymbol{x}_i)\bigg)\bigg(\prod_{a\in\mathcal{A}} f(\tilde{z}_{a,i}|\boldsymbol{x}_i,\boldsymbol{x}_a)\bigg) \times \prod_{j\in\mathcal{D}_i} f(\underline{z}_{i,j}|\boldsymbol{x}_i,\boldsymbol{x}_j) \tag{2}$$

which consists of the prior PDF $f(\boldsymbol{x}_i)$ of agent state i, the likelihood function $f(\tilde{z}_{a,i}|\boldsymbol{x}_i,\boldsymbol{x}_a)$ representing the non-cooperative part and the likelihood function $f(\underline{z}_{i,j}|\boldsymbol{x}_i,\boldsymbol{x}_j)$ representing the cooperative part [1–3]. We use distance measurements to infer the position of the agents. In particular, the distance measurement between two nodes i and j is modelled as

$$z_{i,j} = h(\boldsymbol{x_i},\boldsymbol{x_j}) + n_{i,j} \tag{3}$$

where we have introduced the nonlinear function $h(\boldsymbol{x_i},\boldsymbol{x_j}) = \sqrt{(x_j-x_i)^2+(y_j-y_i)^2}$. The measurement noise $\mathsf{n}_{i,j}$ is assumed iid across i and j, zero-mean, Gaussian with variance σ^2. Note that the measurements model (3), defines the functional form of the likelihood functions $f(\tilde{z}_{a,i}|\boldsymbol{x}_i,\boldsymbol{x}_a)$ and $f(\underline{z}_{i,j}|\boldsymbol{x}_i,\boldsymbol{x}_j)$.

3. REVIEW OF PARTICLE FLOW

Particle flow transfers particles from the prior PDF to the posterior PDF by solving a partial differential equation [14–16, 20]. The particle flow is described by making use of the homotopy property and the Fokker-Planck equation (FPE) [21]. The FPE is used to find a flow of particles that is equivalent to the flow of probability density given by the log-homotopy function for the joint state $\mathbf{x}$, which is described as

$$\log p(\boldsymbol{x},\lambda) = \log f(\boldsymbol{x}) + \lambda \log l(\boldsymbol{x}) - \log K(\lambda) \tag{4}$$

with $\lambda \in [0,1]$ being the introduced pseudo time of the flow process. The prior PDF is given as $f(\boldsymbol{x})$, the likelihood function as $l(\boldsymbol{x}) = f(\boldsymbol{z}|\boldsymbol{x})$ and the evidence as $K(\lambda)$. The posterior PDF at pseudo time λ is written as $p(\boldsymbol{x},\lambda)$. It is assumed that the flow follows a stochastic differential equation of the form of $d\boldsymbol{x} = \boldsymbol{\zeta}(\boldsymbol{x},\lambda)d\lambda + dw$ [14, 15]. The FPE is given as

$$\frac{\partial p(\boldsymbol{x},\lambda)}{\partial\lambda} = -\nabla_{\boldsymbol{x}}^{\mathrm{T}}(p(\boldsymbol{x},\lambda)\boldsymbol{\zeta}(\boldsymbol{x},\lambda)) + \frac{1}{2}\nabla_{\boldsymbol{x}}^{\mathrm{T}}(p(\boldsymbol{x},\lambda)\boldsymbol{Q}(\boldsymbol{x},\lambda))\nabla_{\boldsymbol{x}} \tag{5}$$

with the drift $\boldsymbol{\zeta}(\boldsymbol{x},\lambda)$ and the diffusion term $\boldsymbol{Q}(\boldsymbol{x},\lambda)$. We can determine the function $\boldsymbol{\zeta}(\boldsymbol{x},\lambda)$ of the stochastic differential equation by combining (4) and (5). The left side of (5) can therefore be reformulated as

$$\frac{\partial p(\boldsymbol{x},\lambda)}{\partial\lambda} = p(\boldsymbol{x},\lambda)\left[\log l(\boldsymbol{x}) - \frac{\partial \log K(\lambda)}{\partial\lambda}\right]. \tag{6}$$

It is possible to further expand the divergence term in (5) by making use of the chain rule as

$$\nabla_{\boldsymbol{x}}^{\mathrm{T}}(p(\boldsymbol{x},\lambda)\boldsymbol{\zeta}(\boldsymbol{x},\lambda)) = p(\boldsymbol{x},\lambda)\nabla_{\boldsymbol{x}}^{\mathrm{T}}\boldsymbol{\zeta}(\boldsymbol{x},\lambda) + (\nabla_{\boldsymbol{x}}^{\mathrm{T}}p(\boldsymbol{x},\lambda))\boldsymbol{\zeta}(\boldsymbol{x},\lambda). \tag{7}$$

There are now many ways of how to solve (5) for $\boldsymbol{\zeta}(\boldsymbol{x},\lambda)$. They can be categorized into zero-diffusion, which assumes $\boldsymbol{Q}(\boldsymbol{x},\lambda) = 0$ and nonzero-diffusion. In this paper we only use the zero-diffusion assumption.

3.1. Exact Daum-Huang (EDH) Filter

Assuming zero-diffusion, (5) simplifies to

$$\frac{\partial p(\boldsymbol{x},\lambda)}{\partial\lambda} = -\nabla_{\boldsymbol{x}}^{\mathrm{T}}(p(\boldsymbol{x},\lambda)\boldsymbol{\zeta}(\boldsymbol{x},\lambda))$$

and by neglecting the derivative of the evidence with respect to λ [14], and substituting (6) and (7) into (5), we get

$$\nabla_{\boldsymbol{x}}^{\mathrm{T}}\boldsymbol{\zeta}(\boldsymbol{x},\lambda) = -\log l(\boldsymbol{x}) - (\nabla_{\boldsymbol{x}}\log p(\boldsymbol{x},\lambda))^{\mathrm{T}}\boldsymbol{\zeta}(\boldsymbol{x},\lambda). \tag{8}$$

An analytic solution for $\boldsymbol{\zeta}(\boldsymbol{x},\lambda)$ in (8) can be found for Gaussian distributions [14], which results in the EDH filter [14, 16]. To satisfy these conditions, we approximate the prior PDF as Gaussian distributed where $\boldsymbol{R}$ is the measurement noise covariance matrix and $\boldsymbol{P}$ is the covariance matrix of the joint state. Then a solution for $\boldsymbol{\zeta}(\boldsymbol{x},\lambda)$ can be found in the form of

$$\boldsymbol{\zeta}(\boldsymbol{x}_\lambda,\lambda) = \boldsymbol{A}\boldsymbol{x}_\lambda + \boldsymbol{b} \tag{9}$$

with

$$\begin{aligned}\boldsymbol{A} &= -\frac{1}{2}\boldsymbol{P}\boldsymbol{H}^{\mathrm{T}}(\lambda\boldsymbol{H}\boldsymbol{P}\boldsymbol{H}^{\mathrm{T}}+\boldsymbol{R})^{-1}\boldsymbol{H} \\ \boldsymbol{b} &= (\boldsymbol{I}+2\lambda\boldsymbol{A})[(\boldsymbol{I}+\lambda\boldsymbol{A})\boldsymbol{P}\boldsymbol{H}^{\mathrm{T}}\boldsymbol{R}^{-1}(\boldsymbol{z}+\boldsymbol{\nu})+\boldsymbol{A}\bar{\boldsymbol{x}}_{\lambda=0}]\end{aligned} \tag{10}$$

where $\boldsymbol{\nu} = h(\bar{\boldsymbol{x}}_\lambda) - \boldsymbol{H}\bar{\boldsymbol{x}}_\lambda$ and $\boldsymbol{H} = \frac{\partial h(\boldsymbol{x})}{\partial \boldsymbol{x}}|_{\boldsymbol{x}=\bar{\boldsymbol{x}}_\lambda}$ with $\bar{\boldsymbol{x}}_\lambda$ being the mean value of the state at pseudo time-step λ and the identity matrix $\boldsymbol{I}$ [16]. We use the short hand notation $h(\boldsymbol{x})$ to indicate all measurement hypotheses for connected nodes. A derivation of (9) is given in [20]. The position of each particle in the joint state $\boldsymbol{x}_{\lambda+\Delta}$ at pseudo-time $\lambda+\Delta$ can now be determined as

$$\boldsymbol{x}_{\lambda+\Delta} = \boldsymbol{x}_\lambda + \boldsymbol{\zeta}(\boldsymbol{x}_\lambda,\lambda)\Delta. \tag{11}$$

It is possible to further reduce the computation time of the EDH filter by comparing the rank of $\boldsymbol{R}$ and $\boldsymbol{P}$. If the rank of $\boldsymbol{R}$ is larger than the rank of $\boldsymbol{P}$, (10) is reformulated using the Woodbury matrix identity.

4. PROBLEM FORMULATION AND PROPOSED METHODS

We estimate the state of the agents in a cooperative manner according to the minimum mean-square error estimator [22], which uses the marginal posterior PDF $f(\boldsymbol{x}_i|\mathbf{z})$ as $\hat{\boldsymbol{x}}_i^{\mathrm{MMSE}} = \int \boldsymbol{x}_i f(\boldsymbol{x}_i|\mathbf{z})d\boldsymbol{x}_i$. Since a direct marginalization of the joint posterior (2) is often infeasible, one can use particle-based BP [23, 24] to approximate the marginal PDFs. A drawback of using a particle-based implementation is that for large state dimensions or a highly informative measurement model, particles can collapse after resampling, which is also known as particle degeneracy [25]. We can tackle this problem by using proposal densities as mentioned in [2], but even then, it is not guaranteed that particles will not collapse. In the following, we describe the proposed PF-based method and the naive PF approach that counteracts the particle degeneracy and briefly describe the BP message-passing algorithms we use as a comparison.

4.1. BP for Cooperative Localization

BP is used to approximate the marginal PDFs of the agent states [2]. We use an iterative message passing scheme where the belief of the state of agent i at message passing iteration $u \in \{1, \dots, U\}$ is given as

$$b^{(u)}(\boldsymbol{x}_i) \propto b^{(0)}(\boldsymbol{x}_i) \int \prod_{a \in \mathcal{A}} f(\tilde{z}_{a,i} | \boldsymbol{x}_i, \boldsymbol{x}_a) \times \prod_{j \in \mathcal{D}_i} \int f(\underline{z}_{i,j} | \boldsymbol{x}_i, \boldsymbol{x}_j)\, b^{(u-1)}(\boldsymbol{x}_j)\, d\boldsymbol{x}_j$$

with the initial belief $b^{(0)}(\boldsymbol{x}_i)$ being proportional to the prior PDF $f(\boldsymbol{x}_i)$. The agent marginal PDF $f(\boldsymbol{x}_i|\boldsymbol{z})$ is approximated up to a normalization constant by the belief $b^{(U)}(\boldsymbol{x}_i)$. We define proposal densities for the agent states based on measurements to anchors. They are indicated as

$$\tilde{b}^{(0)}(\boldsymbol{x}_i) \propto b^{(0)}(\boldsymbol{x}_i) \prod_{a \in \mathcal{A}} f(\tilde{z}_{i,a} | \boldsymbol{x}_i, \boldsymbol{x}_a).$$

For each iteration, the belief of agent state i is calculated as

$$b^{(u)}(\boldsymbol{x}_i) \propto \tilde{b}^{(0)}(\boldsymbol{x}_i) \prod_{j \in \mathcal{D}_i} \int f(\underline{z}_{i,j} | \boldsymbol{x}_i, \boldsymbol{x}_j) \times b^{(u-1)}(\boldsymbol{x}_j)\, d\boldsymbol{x}_j. \tag{12}$$

After each iteration u, we approximate the belief of the ith agent state by a resampled set of particles with equal weights as $\{\boldsymbol{x}_i^{(m)}\}_{m=1}^{N_s}$, where N_s is the number of particles. To avoid particle degeneracy after resampling, we can use regularization where we convolve the resampled set of particles with a kernel that could be estimated or predefined [26]. The mth particle $\acute{\boldsymbol{x}}_i^{(m)}$ is drawn from a Gaussian distribution with a mean value of $\boldsymbol{x}_i^{(m)}$ and a variance of σ_k^2.

4.2. BP With Embedded Particle Flow

This approach uses the same BP scheme to approximate the marginal PDF of the state as mentioned in Section 4.1. The only difference is that instead of a point-wise multiplication of the likelihood function, we use particle flow based on the marginal PDFs of the state. In terms of the PF equations, (12) can be written in the form of

$$\boldsymbol{x}_{\lambda+\Delta,i}^{(u)} = \boldsymbol{x}_{\lambda,i}^{(0)} + \boldsymbol{\zeta}(\boldsymbol{x}_{\lambda,i}^{(0)}, \hat{\boldsymbol{x}}_{\lambda=1,i}^{(u-1)}, \lambda)\Delta$$

where $\boldsymbol{x}_{\lambda+\Delta,i}^{(u)}$ indicates the state of agent i at flow-time step $\lambda + \Delta$ and at the uth iteration of the BP algorithm. The initial state $\boldsymbol{x}_{\lambda=0,i}^{(0)}$ is determined by calculating the flow based on the corresponding anchor measurements as explained in Section 4.3. We also define $\hat{\boldsymbol{x}}_{\lambda=1,i}^{(u-1)} = [\boldsymbol{x}_{\lambda=1,j}^{(u-1)}]_{j\in\mathcal{D}_i}$, which indicate the states of the cooperating partner of agent i at the end of their flow ($\lambda = 1$) at the previous iteration $(u-1)$ and

$$\boldsymbol{\zeta}(\boldsymbol{x}_{\lambda,i}^{(0)}, \hat{\boldsymbol{x}}_{\lambda=1,i}^{(u-1)}, \lambda) = \boldsymbol{A}_i \boldsymbol{x}_{\lambda,i}^{(0)} + \boldsymbol{b}_i$$

with $\boldsymbol{A}_i \doteq \boldsymbol{A}(\boldsymbol{x}_{\lambda,i}^{(0)}, \hat{\boldsymbol{x}}_{\lambda=1,i}^{(u-1)}, \lambda)$ and $\boldsymbol{b}_i \doteq \boldsymbol{b}(\boldsymbol{x}_{\lambda,i}^{(0)}, \hat{\boldsymbol{x}}_{\lambda=1,i}^{(u-1)}, \lambda)$. The observation matrix $\hat{\boldsymbol{H}}_i = [\boldsymbol{H}_j]_{j\in\mathcal{D}_i}$ is determined based on the linearization at the mean values of the involved states

$$\boldsymbol{H}_j = \left.\frac{\partial h(\boldsymbol{x}_i, \boldsymbol{x}_j)}{\partial \boldsymbol{x}_i}\right|_{\boldsymbol{x}_i = \bar{\boldsymbol{x}}_{\lambda,i}^{(0)},\ \boldsymbol{x}_j = \bar{\boldsymbol{x}}_{\lambda=1,j}^{(u-1)}} \tag{13}$$

which leads to

$$\begin{aligned}
\boldsymbol{A}_i &= -\frac{1}{2}\boldsymbol{P}_i \hat{\boldsymbol{H}}_i^{\mathrm{T}} (\lambda \hat{\boldsymbol{H}}_i \boldsymbol{P}_i \hat{\boldsymbol{H}}_i^{\mathrm{T}} + \boldsymbol{R})^{-1} \hat{\boldsymbol{H}}_i \\
\boldsymbol{b}_i &= (\boldsymbol{I} + 2\lambda \boldsymbol{A}_i) \Big[(\boldsymbol{I} + \lambda \boldsymbol{A}_i) \boldsymbol{P}_i \hat{\boldsymbol{H}}_i^{\mathrm{T}} \boldsymbol{R}^{-1} (\underline{\boldsymbol{z}}_i - \boldsymbol{\nu}_i) \\
&\quad + \boldsymbol{A}_i \bar{\boldsymbol{x}}_{\lambda=0,i}^{(0)} \Big]
\end{aligned}$$

where $\boldsymbol{\nu}_i = h(\bar{\boldsymbol{x}}_{\lambda,i}^{(0)}, \bar{\hat{\boldsymbol{x}}}_{\lambda=1,i}^{(u-1)}) - \hat{\boldsymbol{H}}_i \bar{\boldsymbol{x}}_{\lambda,i}^{(0)}$, $\underline{\boldsymbol{z}}_i = [\underline{z}_{i,j}]_{j\in\mathcal{D}_i}$ and $\boldsymbol{P}_i$ being the sample based covariance of the ith agent state determined after the first flow based on anchor measurements. The linearization at the mean values in (13) is an additional approximation to reduce the computational complexity. After each message passing iteration u, agent states are resampled.

4.3. Naive Particle Flow

The most straightforward approach for estimating the agent's position with PF is to perform the flow on the joint state with all available measurements from anchors and cooperative partners, which corresponds to solving (1). However, we observe that the flow on the joint state has an inferior performance since the cooperative measurements lead to diverging particles if the prior PDF of the states is uninformative. We solve this problem by letting the particles flow in two steps, equivalent to a factorization into a noncooperative and a cooperative part. At first, we solve (11) using only measurements to anchors and represent it by a resampled set of particles, which defines the new proposal density of the agent states. Based on that proposal distribution, we recalculate $\boldsymbol{P}$ and calculate the cooperative flow by solving (11) using only cooperative measurements and initializing the agent states based on the previously determined proposal density. Even though we perform the flow on the joint state, we resample each state individually at $\lambda = 1$, which neglects the correlation between the states but results in a much better approximation of the marginal PDFs, especially for lower numbers of particles. It is also legitimized by our choice of $\boldsymbol{P}$. It has only entries at the block diagonal, representing the individual states and therefore also neglects the correlations between the states. We chose it in that way since for more extensive networks, the inversion of $\boldsymbol{P}$ can lead to numerical problems, which let the filter diverge—choosing $\boldsymbol{P}$ to be block diagonal solves this problem.

5. EVALUATION OF ALGORITHMS

In this section, we will study the performance of the proposed methods based on simulation in a static 2D scenario for different measurement uncertainties and network sizes. In addition, we will compare it to the state-of-the-art particle-based message-passing algorithms described in Section 4.1. For the BP algorithm with regularization we used $\sigma_k = 0.1$ m. For the following simulations, we use eight anchors and various numbers of agents. The true agent positions are uniformly drawn for each realization on an area of 20 m×20 m.

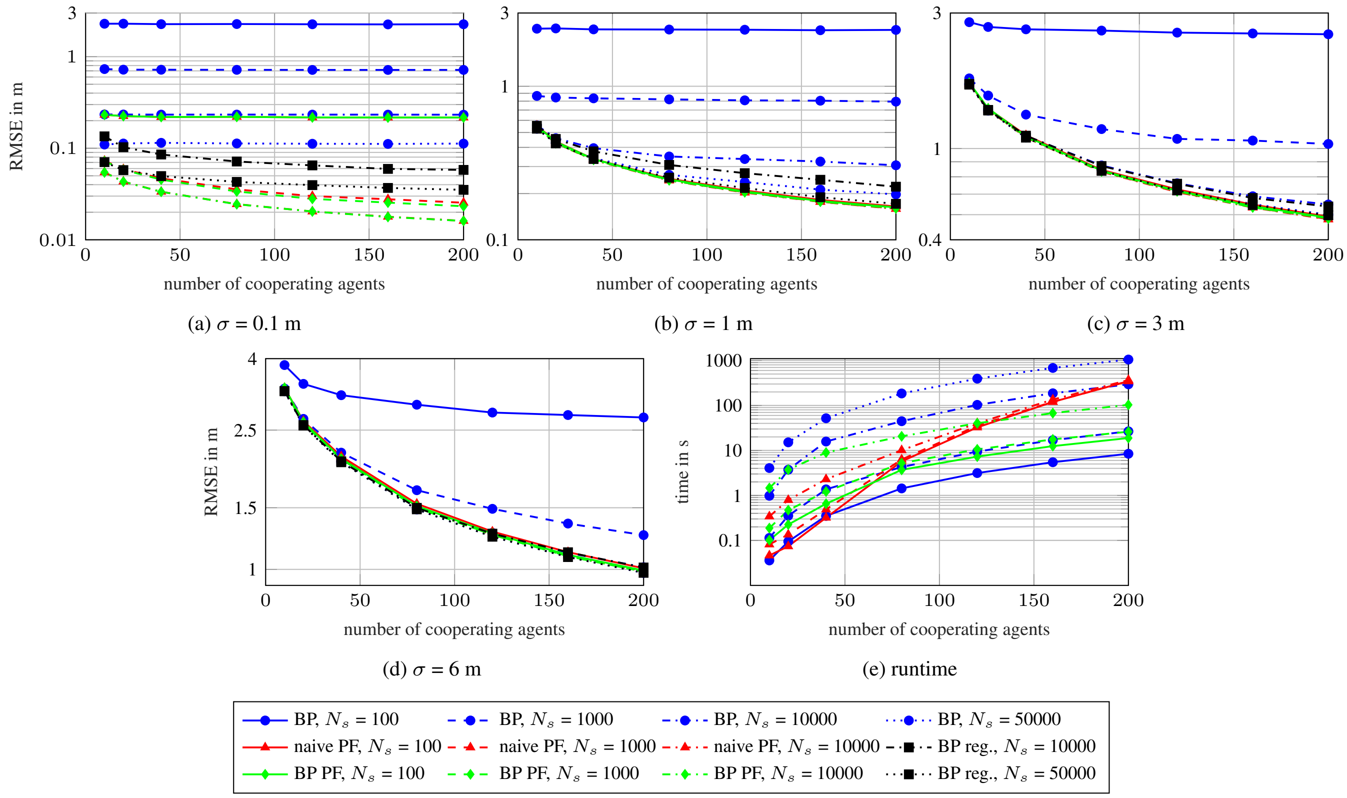

(a) $\sigma = 0.1$ m

(b) $\sigma = 1$ m

(c) $\sigma = 3$ m

(d) $\sigma = 6$ m

(e) runtime

Fig. 1: This figure shows the RMSE in m for the investigated methods described in Section 4. It is evaluated for various numbers of links per agent and for four values of measurement noise. Each point is averaged over 100 simulation runs. In addition, we show the runtime of the different algorithms in seconds.

The support area for initializing the particles is ± 5 m of the agent area. The anchors are placed equally spaced at the boundary of the support area. The results in terms of position root-mean-square error (RMSE) and computation time depending on the different approaches are given in Fig. 1. For a fixed computation time, the PF-based approaches always perform better in our simulations. We can also see that the particle-based BP algorithm would need much more particles to achieve the same accuracy as the PF-based methods with the same amount of particles. This would lead to a huge increase in computation time and memory.

In general, the information in a network increases with an increasing number of links, resulting in higher estimation accuracy. Nevertheless, we see especially for highly informative measurement models and specific numbers of particles a constant RMSE with an increasing number of links. This is because the agent states are not sufficiently represented with that amount of particles to capture the information gain. We also show, based on simulations, that the two proposed methods are equally accurate, but there is a trade-off in computation time regarding the number of links per agent. For smaller networks or a small number of links, the *naive particle flow* is faster, whereas for large networks or a large number of links per agent *BP with embedded particle flow* is preferred. This is because the matrix inversion in (10) is getting more time-consuming for larger state dimensions. These approaches can be easily extended to other particle flow filters like the Localized-Exact-Daum-Huang filter [16] or stochastic particle flow filter as described in [27, 28]. In general, those methods perform better in terms of accuracy since multi-modal distributions can be correctly represented. However, the computational complexity increases since the observation matrix $\boldsymbol{H}$ is evaluated at each particle. The computation time of the standard BP algorithm with regularization is not shown in Fig. 1e since it has approximately the same runtime as without regularization.

6. CONCLUSION

This paper introduced a new method for cooperative localization in large-scale networks. Our approach combines belief propagation (BP) with particle flow (PF) to avoid particle degeneracy. The proposed PF-BP method was evaluated numerically in scenarios with up to 200 cooperative agents. The simulation results demonstrated improved accuracy and reduced runtime compared to state-of-the-art particle-based BP algorithms. Possible directions of future research include an extension to dynamic networks as well as self-measurements of the agent state provided by an intertial measurement unit.

7. ACKNOWLEDGEMENT

DISTRIBUTION STATEMENT A: Approved for public release. Distribution is unlimited. Any opinions, findings, conclusions, or recommendations expressed in this material are those of the author(s) and do not necessarily reflect the views of the Under Secretary of Defense for Research and Engineering.

8. REFERENCES

[1] H. Wymeersch, J. Lien, and M. Z. Win, "Cooperative localization in wireless networks," *Proc. IEEE*, vol. 97, no. 2, pp. 427 –450, Feb. 2009.

[2] F. Meyer, O. Hlinka, H. Wymeersch, E. Riegler, and F. Hlawatsch, "Distributed localization and tracking of mobile networks including noncooperative objects," *IEEE Trans. Signal Inf. Process. Netw.*, vol. 2, no. 1, pp. 57–71, Mar. 2016.

[3] L. Wielandner, E. Leitinger, and K. Witrisal, "RSS-based cooperative localization and orientation estimation exploiting antenna directivity," *IEEE Access*, vol. 9, pp. 53 046–53 060, Mar. 2021.

[4] J. Kulmer, E. Leitinger, S. Grebien, and K. Witrisal, "Anchorless cooperative tracking using multipath channel information," *IEEE Trans. Wireless Commun.*, vol. 17, no. 4, pp. 2262–2275, Apr. 2018.

[5] S. Zhang, E. Staudinger, T. Jost, W. Wang, C. Gentner, A. Dammann, H. Wymeersch, and P. A. Hoeher, "Distributed direct localization suitable for dense networks," *IEEE Trans. Aerosp. Electron. Syst.*, vol. 56, no. 2, pp. 1209–1227, 2020.

[6] C. Gentner, W. Jost, T.and Wang, S. Zhang, A. Dammann, and U. C. Fiebig, "Multipath assisted positioning with simultaneous localization and mapping," *IEEE Trans. Wireless Commun.*, vol. 15, no. 9, pp. 6104–6117, Sept. 2016.

[7] E. Leitinger, F. Meyer, F. Hlawatsch, K. Witrisal, F. Tufvesson, and M. Z. Win, "A belief propagation algorithm for multipath-based SLAM," *IEEE Trans. Wireless Commun.*, vol. 18, no. 12, pp. 5613–5629, Dec. 2019.

[8] F. Meyer and J. L. Williams, "Scalable detection and tracking of geometric extended objects," *IEEE Trans. Signal Process.*, vol. 69, pp. 6283–6298, Dec. 2021.

[9] E. Leitinger, S. Grebien, and K. Witrisal, "Multipath-based SLAM exploiting AoA and amplitude information," in *Proc. IEEE ICCW-19*, Shanghai, China, May 2019, pp. 1–7.

[10] H. Kim, K. Granström, L. Gao, G. Battistelli, S. Kim, and H. Wymeersch, "5G mmWave cooperative positioning and mapping using multi-model PHD filter and map fusion," *IEEE Trans. Wireless Commun.*, vol. 19, no. 6, pp. 3782–3795, Mar. 2020.

[11] E. Leitinger and F. Meyer, "Data fusion for multipath-based SLAM," in *Proc. Asilomar-20*, Pacifc Grove, CA, USA, Oct. 2020.

[12] C. Musso, N. Oudjane, and F. Le Gland, "Improving regularised particle filters," in *Sequential Monte Carlo methods in practice*. Springer, New York, NY, 2001, pp. 247–271.

[13] M. Arulampalam, S. Maskell, N. Gordon, and T. Clapp, "A tutorial on particle filters for online nonlinear/non-Gaussian Bayesian tracking," *IEEE Trans. Signal Process.*, vol. 50, no. 2, pp. 174–188, Feb. 2002.

[14] F. Daum, J. Huang, and A. Noushin, "Exact particle flow for nonlinear filters," in *Proc. SPIE-10*, vol. 7697, Apr. 2010, p. 769704.

[15] F. Daum and J. Huang, "Particle flow with non-zero diffusion for nonlinear filters," in *Proc. SPIE-13*, vol. 8745, May 2013, p. 87450P.

[16] Y. Li and M. Coates, "Particle filtering with invertible particle flow," *IEEE Trans. Signal Process.*, vol. 65, no. 15, pp. 4102–4116, May 2017.

[17] Y. Li, S. Pal, and M. J. Coates, "Invertible particle-flow-based sequential MCMC with extension to Gaussian mixture noise models," *IEEE Trans. Signal Process.*, vol. 67, no. 9, pp. 2499–2512, 2019.

[18] F. Meyer, T. Kropfreiter, J. L. Williams, R. A. Lau, F. Hlawatsch, P. Braca, and M. Z. Win, "Message passing algorithms for scalable multitarget tracking," *Proc. IEEE*, vol. 106, no. 2, pp. 221–259, Feb. 2018.

[19] W. Zhang and F. Meyer, "Graph-based multiobject tracking with embedded particle flow," in *Proc. IEEE RadarConf-21*, Atlanta, GA, USA, 2021, pp. 1–6.

[20] D. F. Crouse and C. Lewis, "Consideration of particle flow filter implementations and biases," Naval Research Lab., Washington DC, United States, Tech. Rep., 2020.

[21] H. Risken, "Fokker-Planck equation," in *The Fokker-Planck Equation*. Springer, 1996, pp. 63–95.

[22] S. M. Kay, *Fundamentals of Statistical Signal Processing: Estimation Theory*. Upper Saddle River, NJ, USA: Prentice Hall, 1993.

[23] F. Kschischang, B. Frey, and H.-A. Loeliger, "Factor graphs and the sum-product algorithm," *IEEE Trans. Inf. Theory*, vol. 47, no. 2, pp. 498–519, Feb. 2001.

[24] H.-A. Loeliger, "An introduction to factor graphs," *IEEE Signal Process. Mag.*, no. 1, pp. 28–41, Jan. 2004.

[25] T. Bengtsson, P. Bickel, and B. Li, "Curse-of-dimensionality revisited: Collapse of the particle filter in very large scale systems," in *Probability and statistics: Essays in honor of David A. Freedman*. Institute of Mathematical Statistics, 2008, pp. 316–334.

[26] F. Meyer, H. Wymeersch, M. Frohle, and F. Hlawatsch, "Distributed estimation with information-seeking control in agent networks," *IEEE J. Sel. Areas Commun.*, vol. 33, no. 11, pp. 2439–2456, Nov. 2015.

[27] F. Daum, J. Huang, and A. Noushin, "Generalized Gromov method for stochastic particle flow filters," in *Proc. SPIE-17*, vol. 10200, May 2017, p. 102000I.

[28] ——, "New theory and numerical results for Gromov's method for stochastic particle flow filters," in *Proc. FUSION-18*, Cambridge, UK, Jul. 2018, pp. 108–115.